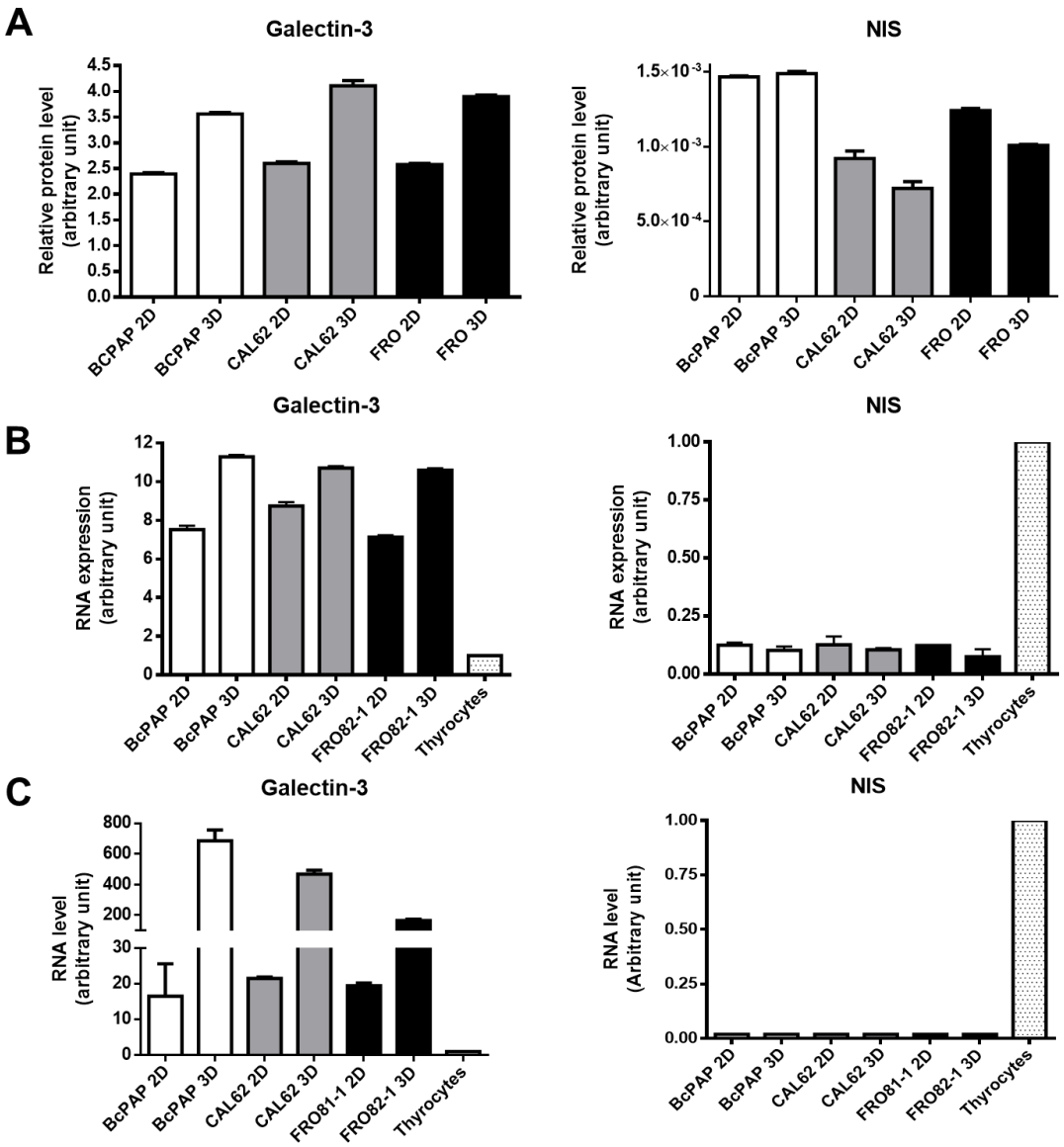

Supplemental Figure 1. Characterization of Gal-3 and NIS expression in the selected cell lines. (**A**) Relative densitometric analysis of bands visualized for gal-3 and NIS expression via western blot normalizing for the signal related to GADPH. (**B**) Relative intensity measurement of the bands visualized for cDNA sequences encoding for Gal-3 and NIS analyzed via PCR. WB and PCR analysis were repeated at least 5 times, each test in triplicate. (**C**) Gal-3 and hNIS gene expression analysis evaluated via qPCR on cDNA derived from total RNA extracted from 2D and 3D cell cultures. Total RNA extract from human thyrocytes (Takara Bio Europe) was used as reference. Data from qPCR were analyzed using $\Delta\Delta C_t$ method.

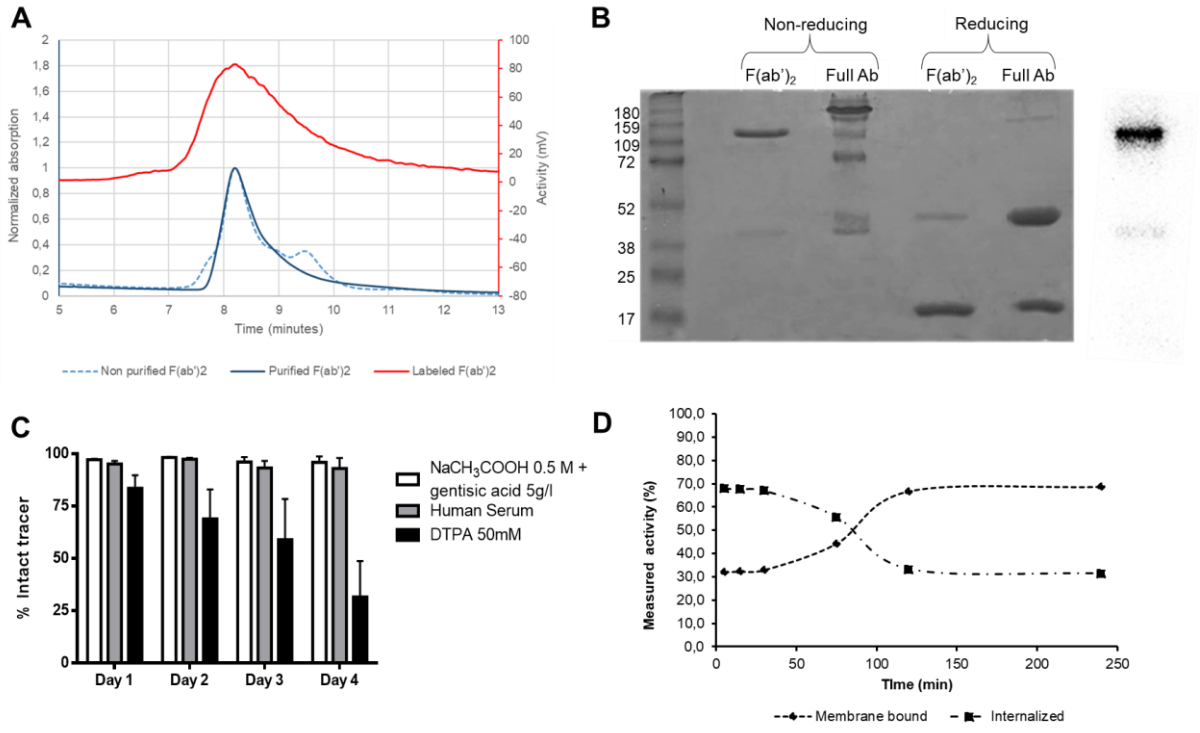

Supplemental Figure 2. *In vitro* characterization of ^{89}Zr-DFO-aGal3-F(ab')$_2$ tracer. (**A**) The radiochemical purity measured via radio-HPLC analysis was > 98%, with radioactivity associated with the peak of F(ab')$_2$ (t_R= 8.3 min.) in UV profile. (**B**) The integrity of the F(ab')$_2$ to gal-3 after conjugation and radiolabeling was confirmed via SDS-PAGE carried out under reducing and non-reducing condition, followed by and autoradiography analysis of the radiolabeled F(ab')$_2$. (**C**) The stability of ^{89}Zr-labelled F(ab')$_2$ to gal-3 in different storage solutions were tested. Aliquots of ^{89}Zr-DFO-aGal3-F(ab')$_2$ probe (1 µl) were taken from each storage solution at different time point, spotted onto a TLC silica gel strip and developed using 0.02 M citrate buffer with 50mM DTPA (pH 5.0) as solvent. ^{89}Zr-labelled F(ab')$_2$ to gal-3 was incubated in 50 mM DTPA solution to determine transchelation effect. Analysis were repeated at least three times, each time in triplicate. Data are presented as mean±SD. (**D**) Internalization test of ^{89}Zr-DFO-aGal3-F(ab')$_2$ on 2D cultures. Membrane bound and internalized activity measured at different time points.

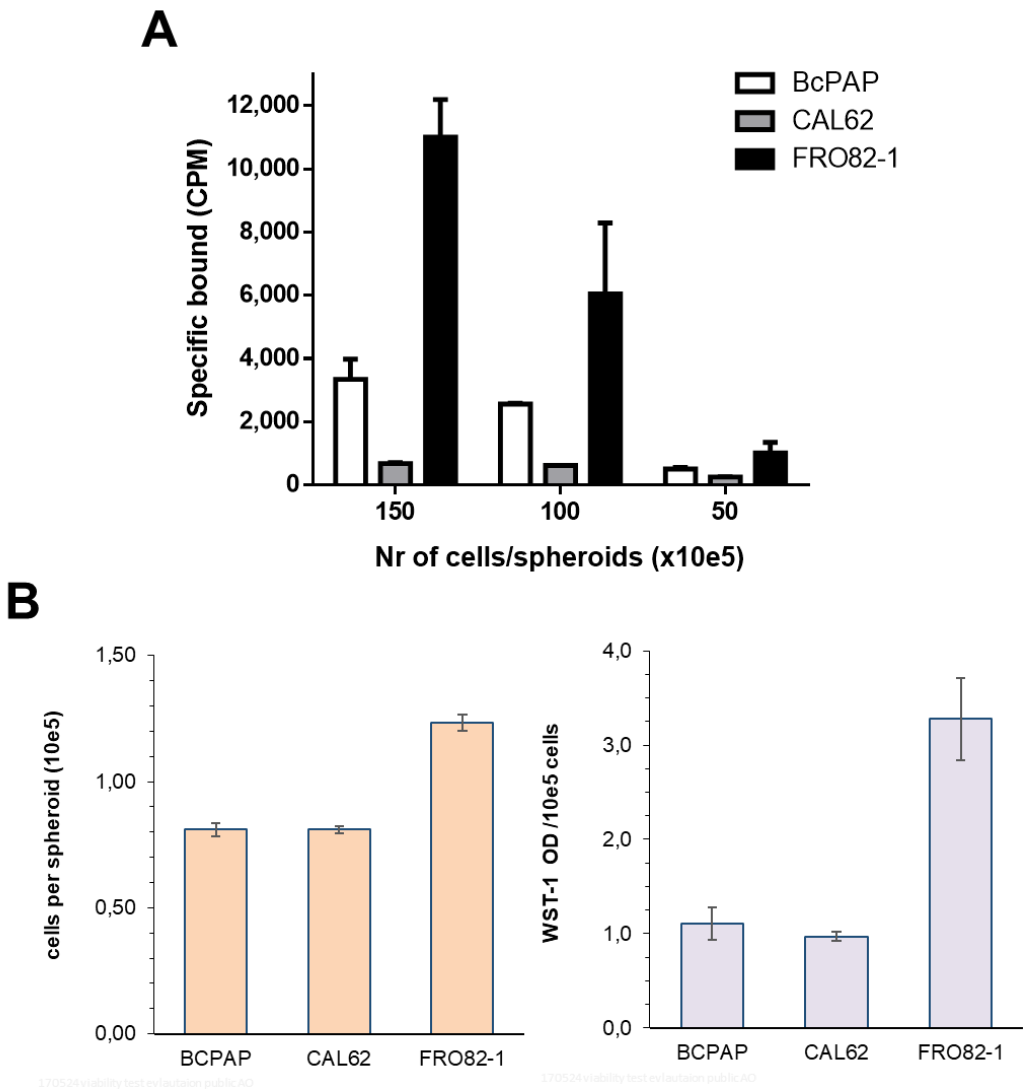

Supplemental Figure 3. Binding and viability tests on tumor spheroids. (**A**) ^{89}Zr-DFO-aGal3-F(ab')$_2$ binding on 3D tumor spheroids, assessed in presence or absence of excess of aGal3-F(ab')$_2$ to evaluate unspecific binding. Data representative of three independent experiments performed each time in triplicate and are expressed as mean±SD. (**B**) Number of cells counted (x100k) per spheroids/aggregates after three days of incubation of 10e5 cells under non-adhesive conditions (upper graph). Metabolic activity evaluated via WST-1 reduction measured as OD450nm-OD630nm (lower graph).

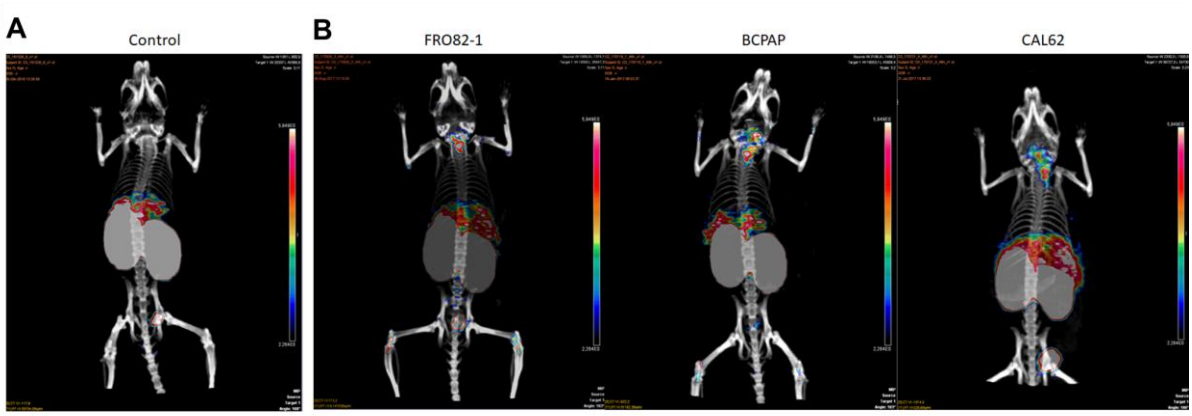

Supplemental Figure 4. In vivo ^{89}Zr-DFO-F(ab')$_2$ to gal-3 tumor accumulation. Maximum Imaging Projection (MIP) images of static PET/CT scans acquired at 48h post injection of 2.22 MBq (60 µCi) ^{89}Zr-DFO-aGal3-F(ab')$_2$. (**A**) No specific tracer accumulation was present in the neck region in healthy control mice, (**B**) vice versa, high tumor to background contrast in the region of neck is showed in each orthotopic model with detailed information about tumor position. Images were analyzed using Inveon Research Workplace software (Siemens, Knoxville, TN).

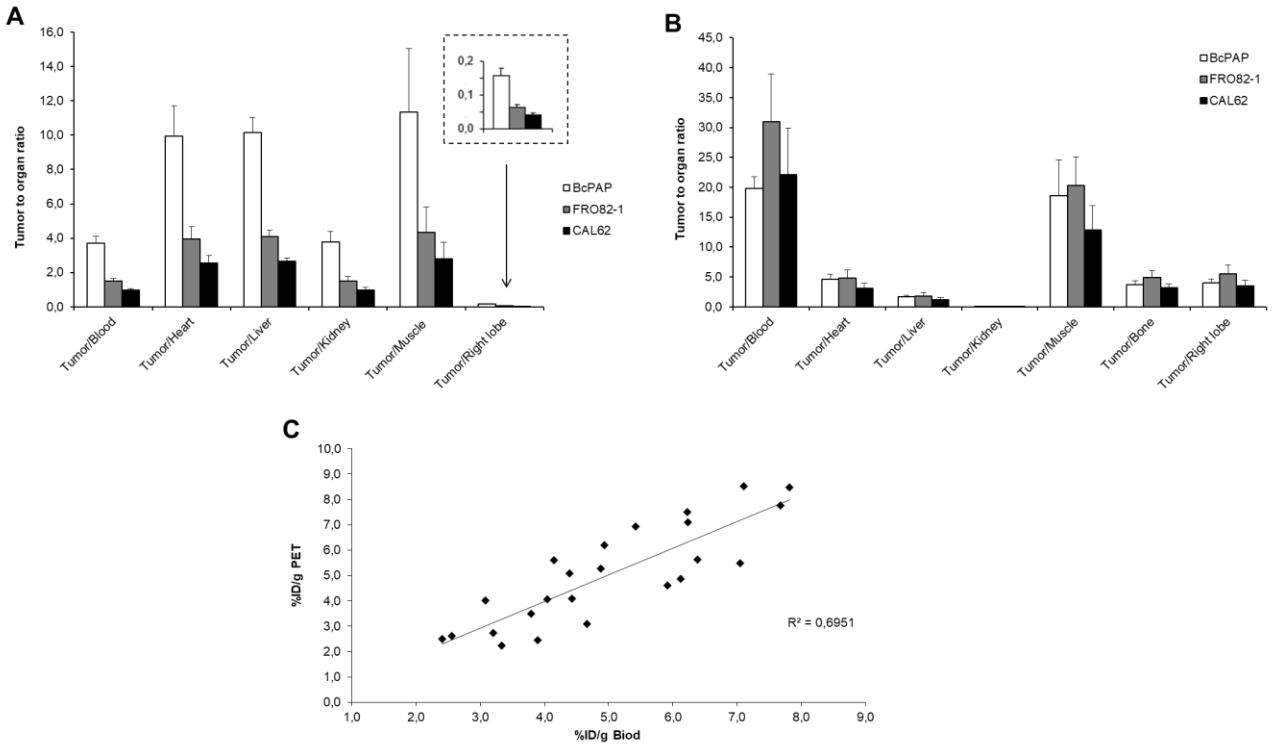

Supplemental Figure 5. Biodistribution analysis of ^{124}I versus ^{89}Zr-DFO-aGal3-F(ab')$_2$. ^{124}I (**A**) and ^{89}Zr-DFO-aGal3-F(ab')$_2$ (**B**) accumulation ratio in left lobe/right lobe. Radioactivity accumulation was calculated as mean+/-SD. (**C**) *In vivo* versus *ex vivo* ^{89}Zr-DFO-F(ab')$_2$ to gal-3 tumor accumulation analysis. Image-derived uptake calculation and ex vivo accumulation analyses were compared for all the mice investigated in this work. For *in vivo* tumor uptake analysis, images were analyzed using Inveon Research Workplace software (Siemens, Knoxville, TN). An arbitrary regions of interest (ROI) was drawn manually on the left side of the trachea encompassing the tumor signal. The radioactivity present in each ROI was determined using a threshold of 50%. The %ID/g was calculated as a ratio of mean radioactivity in each ROI (MBq) per gram of tumor tissue (weighted post-mortem) and radioactivity (MBq) injected in the whole body. *Ex vivo* accumulation data were obtained from biodistribution studies by counting the tumors in γ-counter. A correlation equal to R^2=0.69 was found between the two tracer accumulation analysis. Ten mice per each group were analyzed using both approaches. Data are presented without taking into account the tumor type analyzed.

Gene	Sequence 5'-3'
GAPDH	Sense: GAGTCAACGGATTTGGTCGT Antisense: TTGATTTTGGAGGGATCTCG
NIS	Sense: CTGCCCCAGACCAGTACATGCC Antisense: TGACGGTGAAGGAGCCCTGAAG
Gal-3	Sense: GCCTCGCATGCTGATAACAA Antisense: ACCGACTGTCTTTCTTCCCT

Supplemental Table 1. Primers used for Gal-3 and hNIS gene expression analysis via qPCR. GAPDH was used as housekeeping genes.

Tumor/organ ratio	BcPAP (*n* = 10)	FRO82-1 (*n* = 10)	CAL62 (*n* = 10)
Tumor/blood	3.71 ± 0.40	1.51 ± 0.16	0.97 ± 0.10
Tumor/heart	9.93 ± 1.78	4.04 ± 0.72	2.59 ± 0.46
Tumor/liver	10.16 ± 0.85	4.13 ± 0.35	2.65 ± 0.22
Tumor/kidney	3.77 ± 0.60	1.53 ± 0.24	0,99 ± 0.16
Tumor/muscle	11.34 ± 3.70	4.61 ± 1.50	2.96 ± 0.97
Left/Right lobe	0.16 ± 0.02	0.06 ± 0.01	0.04 ± 0.01

Supplemental Table 2. Tumor/organs accumulation ratio analysis for ^{124}I in thyroid orthotopic models. The tumor-to-organ ratio values were calculated from γ-counter measurements of selected organs analyzed at 1hr after ^{124}I injection. A positive tumor/organ ratio was measured for all selected organs. A very low left/right lobe ratio was measured for all models investigated, due to the low accumulation of ^{124}I in the tumor bearing left lobe compared to the right normal thyroid lobe. These results correlate well with the very low NIS expression found out in western blot and PCR analysis. Data are expressed as mean %ID/g ± SD.

Tumor/organ ratio	BcPAP (*n* = 10)	FRO82-1 (*n* = 10)	CAL62 (*n* = 10)
Tumor/blood	19.77 ± 1.95	30.99 ± 7.96	22.14 ± 7.82
Tumor/heart	4.65± 0.81	4.79± 1.43	3.05± 0.89
Tumor/liver	1.69± 0.24	1.84± 0.52	1.17± 0.32
Tumor/kidney	0.06 ± 0.03	0.08 ± 0.03	0,05 ± 0.01
Tumor/muscle	18.62 ± 6.01	20.26 ± 4.86	12.88 ± 4.08
Tumor/bone	3.71 ± 0.67	4.94 ± 1.16	3.15 ± 0.74
Left/Right lobe	4.02 ± 0.65	5.49 ± 1.47	3.48 ± 0.93

Supplemental Table 3. Tumor/organs accumulation analysis of ^{89}Zr-DFO-aGal3-F(ab')$_2$ in thyroid orthotopic models. The tumor-to-organ ratio values were calculated from γ-counter measurements of activity accumulated in selected organs measured at 48hr after ^{89}Zr-DFO-aGal3-F(ab')$_2$ injection. A positive tumor/organ ratio was measured for all selected organs, except for the liver and kidneys due to metabolism and excretion of the tracer. The positive ratio tumor/muscle indicate a high *in vivo* stability of the tracer, with very low free ^{89}Zr present in circulation and consequent low bone uptake. A high ratio left/right thyroid lobe was measured for all models investigated. Data are expressed as mean %ID/g ± SD.